THE ASTROPHYSICAL JOURNAL, 302:693–700, 1986 March 15

COMPARISON OF 2.1 AND 3.8 MICRON LINE PROFILES OF SHOCKED H_2 IN THE ORION MOLECULAR CLOUD

T. R. GEBALLE[1]
Kapteyn Astronomical Institute, Rijksuniversiteit te Groningen, and United Kingdom Infrared Telescope
S. E. PERSSON[1]
Mount Wilson and Las Campanas Observatories of the Carnegie Institution of Washington
THEODORE SIMON[1]
Institute for Astronomy, University of Hawaii
CAROL J. LONSDALE[1]
Department of Astronomy, University of California at Los Angeles
AND
P. J. MCGREGOR[2]
Mount Wilson and Las Campanas Observatories of the Carnegie Institution of Washington
Received 1985 June 17; accepted 1985 September 12

ABSTRACT

Velocity profiles of the 2.12 μm 1–0 *S*(1) and 3.81 μm 1–0 *O*(7) lines of H_2 have been measured at a number of locations in the shocked gas region of the Orion molecular cloud. In the center of this region, the *O*(7) lines have relatively stronger wings than do the *S*(1) lines. With respect to the velocity of the molecular cloud, blueshifted *O*(7) emission is more prominent than redshifted emission, as is the case for the *S*(1) line. These data imply that although some extinction through the outflow is present, the asymmetries in the H_2 lines are due in part to actual line-of-sight distributions of velocities within the shocked gas. These distributions appear consistent with the sense of the bipolar outflow observed in millimeter CO lines between the lobes of H_2 line emission. Scattering of H_2 line photons off moving dust grains apparently is not the major cause of the broad-line emission within the lobes.

Subject headings: infrared: spectra — interstellar: molecules — line formation — line profiles — nebulae: Orion Nebula — shock waves

I. INTRODUCTION

Line emission from shocked molecular hydrogen is a common feature near high-velocity molecular outflows associated with embedded pre–main-sequence stars. A proper understanding of the H_2 line-emission phenomenon depends upon mapping of H_2 line profiles at high spectral resolution. To date, the only object in which this has proven possible is the Orion molecular cloud (OMC-1).

In OMC-1, measurements by Nadeau and Geballe (1979), Nadeau, Geballe, and Neugebauer (1982), and Scoville *et al.* (1982) have demonstrated that the velocity profiles of the 1–0 *S*(1) line at 2.12 μm vary in shape from approximately symmetric to a severe blue asymmetry, with velocity extrema of about +60 km s^{-1} and −100 km s^{-1} (LSR) and line-peak velocities near that of the surrounding unshocked cloud, +9 km s^{-1} (LSR). In contrast, the millimeter CO profiles from the core (BN/KL region) of OMC-1 were found to be approximately symmetric and to extend 100 km s^{-1} to either side of +9 km s^{-1} (Kwan and Scoville 1976; Zuckerman, Kuiper, and Rodriguez Kuiper 1976). They imply that the velocity of the outflow source is very close to the cloud velocity.

The blue asymmetry of the H_2 *S*(1) line profiles was interpreted by Nadeau and Geballe (1979) and by subsequent investigators as being due to extinction existing within the molecular flow and thus between shocked regions on the near and far sides of the flow. Roughly two magnitudes of internal extinction at 2.12 μm could suppress the redshifted *S*(1) emission on the far side and alter intrinsically symmetric line profiles to the observed degree of asymmetry. If this explanation is correct, profiles of longer wavelength lines, where the extinction is less, should appear more symmetric and possibly broader than the 2.12 μm line. Scoville *et al.* (1982) found that the blue wings of the 1–0 *Q*(3) (2.42 μm) and *S*(1) line profiles at Peak 1 and Peak 5 (designation of Beckwith *et al.* 1978) are stronger relative to line center than are the blue wings of the shorter wavelength *S*(1) profiles and concluded that the blueshifted emission is located interior to, and is more highly obscured than, the emission at line center. However, they were unable to obtain accurate measurements of redshifted *Q*(3) line emission because of telluric absorption of that part of that line. Evidence for internal obscuration at a few positions also has been reported by Beck *et al.* (1982), based on their observations of the 12.3 μm pure rotational *S*(2) line profiles. However, since the *S*(2) line has a significantly lower upper-state energy than does the 1–0 *S*(1) line, these observations do not sample the same gas as do observations of the *S*(1) line. Thus, further tests are needed.

An important development in the understanding of the diverse phenomena in the Orion molecular cloud was the determination by Erickson *et al.* (1982) that the outflow seen in the millimeter CO lines is bipolar. The degree of collimation of the outflowing gas is not well determined, but its existence

[1] Visiting Astronomer at the Infrared Telescope Facility which is operated by the University of Hawaii under contract from the National Aeronautics and Space Administration.
[2] Mount Stromlo and Siding Spring Observatories, Australian National University.

suggests that the explanation for the $S(1)$ line profiles may result wholly or in part from an intrinsic bipolar velocity effect and not from internal obscuration.

We report here high spectral resolution observations of both the H_2 1–0 $S(1)$ and 1–0 $O(7)$ line at a number of positions in OMC-1. The $O(7)$ line at 3.81 μm was chosen for the following reasons. (1) Its upper level energy is similar to that of the 1–0 $S(1)$ transition and therefore the two lines are emitted by very nearly the same gas. (2) Its wavelength is sufficiently longward of 2.12 μm that any extinction through the line-emitting region should be reduced significantly. (3) It is only marginally attenuated by telluric absorption lines, and fluctuations in the thermal background are not as severe as at longer (12.3 μm) wavelengths in limiting the sensitivity of the measurements. Therefore, observations of the $O(7)$ line, together with those of the $S(1)$ line, can provide useful insight into the physical structure of the shocked gas region.

II. OBSERVATIONS AND VELOCITY CALIBRATION

The observations were made at the NASA 3 m infrared telescope (IRTF) of the Mauna Kea Observatory on the nights of 1981 December 5–7, using the Fabry-Perot and cold grating spectrometer described by Persson, Geballe, and Baas (1982). Different Fabry-Perot interferometers were required to observe the two lines; each was set to a velocity resolution of 22 ± 2 km s^{-1} at the frequency of the line it was to measure. The entrance aperture of the grating spectrometer corresponded to a circular field of view of 6".5 at the IRTF. Standard chopping and beam-switching techniques were employed, using an east-west beam separation of $\sim 45''$.

Alignment and stability of each interferometer was monitored by recording interference fringes from a 6328 Å HeNe laser during data taking and by observing emission lines from discharge lamps. In the case of the $S(1)$ line, whose rest frequency is accurately known, an absolute velocity scale, accurate to ± 2 km s^{-1}, was determined from the discharge lamp observations. Velocity calibration was not directly possible for the $O(7)$ line spectra, because the rest frequency of that line was not known to sufficient accuracy at the time of the observations. In order to obtain a velocity scale, we have assumed that the peak emissions in the $O(7)$ lines at Peaks 2 and 5 occur at the same velocities as the bright narrow peaks seen in the $S(1)$ line at those locations. Our measurements of the $S(1)$ line showed that at Peak 2 the LSR velocity of maximum intensity, +13 km s^{-1}, is redshifted by 2 ± 2 km s^{-1} relative to that at Peak 5. The $S(1)$ spectra of Nadeau, Neugebauer, and Geballe (1982) and Scoville *et al.* (1982) are in agreement with this shift. In our IRTF measurements of the $O(7)$ line a surprisingly large redshift of ~ 10 km s^{-1} was found at Peak 2 relative to Peak 5. It appeared possible that instability of the interferometer during our $O(7)$ measurements of Peak 2 led to unreliable data there or that the larger than expected velocity shift was a consequence of low signal-to-noise ratios on the $O(7)$ lines. In order to resolve the uncertainty, new measurements of the $O(7)$ line were carried out in 1983 at the United Kingdom Infrared Telescope by one of us (TRG). From the new measurements, the peak line intensity at Peak 2 was found to be redshifted by 5 ± 4 km s^{-1} relative to Peak 5, a result consistent with that obtained for the $S(1)$ line.

Obviously, there is some uncertainty as to the proper velocity scale for the $O(7)$ spectra. Because both the $O(7)$ and the $S(1)$ lines have narrow peaks at Peak 2 and Peak 5, we regard as sound the assumption that the peak $O(7)$ line emissions are at the same velocities as the $S(1)$ emissions at these two locations. The IRTF $O(7)$ measurement at Peak 5 probably is more reliable than that at Peak 2 because of the somewhat higher signal-to-noise ratio and the lack of a strong continuum at the former position. Therefore, rather than splitting the velocity difference between the two positions, we have defined the LSR velocity of maximum line emission at Peak 5 to be +11 km s^{-1} [the same as that observed in the $S(1)$ line there]. This definition is at the high end of the range of velocities, consistent with our assumption and with the uncertainties, and has a formal uncertainty of (-7, $+3$) km s^{-1}. Errors of this magnitude will not change the sense of the results presented below or the sense of the following discussion. We note that when using this definition there is good agreement of $O(7)$ and $S(1)$ line peaks at the other observed positions.

Spectra of the $S(1)$ and $O(7)$ lines were obtained at five positions: Peak 1, Peak 2, Peak 5, IRc2, and IRc4. These spectra, binned in 10 km s^{-1} wide intervals, are shown in Figure 1. The spectra at Peak 1 are also displayed in Figure 2. For several of the $O(7)$ spectra, most notably those at IRc2 and IRc4, linear and nearly flat baselines have been subtracted from the original spectra. Spectra of bright stars were also measured; these show that the atmospheric transmission near the H_2 lines is excellent and that ratios are not required. The H_2 spectra are not flux-calibrated and have been normalized to the same peak line intensity in Figure 1 to allow easier comparison of the line profiles. The fractional line intensities in 50 km s^{-1} wide bands centered at 0, ± 50, and ± 100 km s^{-1} from the local cloud velocity of +9 km s^{-1} (LSR) are tabulated in Table 1, along with other relevant line parameters.

III. RESULTS

The H_2 $S(1)$ line profiles shown in Figure 1 and quantitatively described in Table 1 are generally consistent with those obtained by Nadeau, Geballe, and Neugebauer (1982) and by Scoville *et al.* (1982). The narrowest lines are found farthest from center of the H_2–line-emitting region. Those closer in tend to have peaks which are blueshifted relative to the 9 km s^{-1} (LSR) velocity of the Orion molecular cloud and have asymmetric line profiles with excess line emission on their blue sides. The most extreme velocities are found at Peak 1, where the blue wing extends at least to -100 km s^{-1} and the red wing at least to +60 km s^{-1}. Also striking are the sharp and nearly unresolved red edges of the $S(1)$ line profiles at IRc2 and IRc4.

The principal difference between the $O(7)$ and $S(1)$ profiles concerns the fraction of intensity in the line center versus in the wings. The velocities of the peaks of the $O(7)$ lines are equal to those of the $S(1)$ line to within the uncertainties, but at four of the five positions the fraction of the total line intensity within the central 50 km s^{-1} of the $O(7)$ line is less than that for the $S(1)$ line (see Table 1). The largest differences in line shape are at Peak 1 and IRc2, where the full widths at half-maximum of the $O(7)$ lines are significantly greater than those of the $S(1)$ line.

Nonetheless, a significant result of these measurements is that there is no large difference between $O(7)$ and $S(1)$ lines in the degree of asymmetry at the three central positions. *Here we are concerned with asymmetry with respect to the local cloud velocity of +9 km s*$^{-1}$ *(LSR)* and not with respect to the different velocities of the line peaks at the different locations. In this sense, Peak 1, IRc2, and IRc4 maintain distinct blue asymmetries in the $O(7)$ line, as is shown in Table 1. At IRc4 the

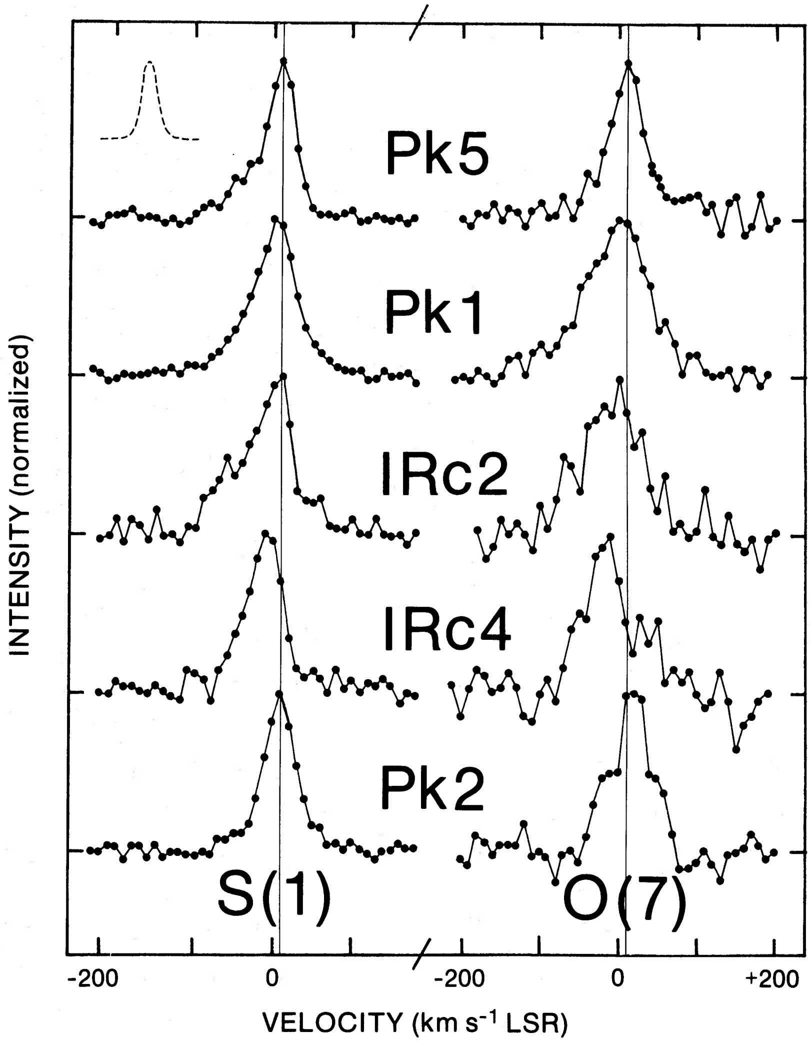

FIG. 1.—Spectra of 1–0 $O(7)$ and $S(1)$ lines at a number of positions in OMC-1. Beam diameter was 6″.5, and velocity resolution, shown in upper left panel, was 22 km s^{-1}. All spectra are normalized to same peak intensity. Linear baselines were subtracted from several of the $O(7)$ spectra. Light, vertical lines are at +9 km s^{-1} (LSR). Noise may be estimated from the baseline fluctuations.

TABLE 1

H_2 $S(1)$ AND $O(7)$ LINE PARAMETERS

POSITION $\Delta\alpha$, $\Delta\delta$[a]	LINE	V_{peak} km s^{-1} LSR	FWHM[b] km s^{-1}	FRACTION OF INTENSITY IN VELOCITY INTERVAL (km s^{-1} LSR) $V < -66$	$-66 < V < -16$	$-16 < V < 34$	$34 < V < 84$	$V > 84$	$\pm\sigma$
Peak 5	$S(1)$	+11	40 (30)	0.03	0.21	0.64	0.10	0.02	±0.01
−4.4, 27.0	$O(7)$	+11	45 (35)	0.05	0.15	0.57	0.16	0.07	±0.04
Peak 1	$S(1)$	+5	60 (50)	0.06	0.23	0.55	0.14	0.02	±0.01
−7.5, 14.8	$O(7)$	+5	85 (75)	0.07	0.27	0.45	0.16	0.03	±0.03
IRc2...................	$S(1)$	+5	60 (50)	0.08	0.29	0.52	0.11	0.01	±0.03
6.0, −7.0	$O(7)$	0	85 (75)	0.11	0.32	0.40	0.13	0.05	±0.05
IRc4...................	$S(1)$	−5	50 (40)	0.02	0.32	0.56	0.07	0.04	±0.03
1.3, −11.4	$O(7)$	−10	50 (40)	0.01	0.40	0.39	0.17	0.03	±0.06
Peak 2	$S(1)$	+13	45 (35)	0.00	0.13	0.67	0.18	0.02	±0.01
22.4, −16.5	$O(7)$	+20	50 (40)	0.00	0.13	0.67	0.22	−0.03	±0.05

[a] In arc seconds, from BN.
[b] Deconvolved values in parentheses.

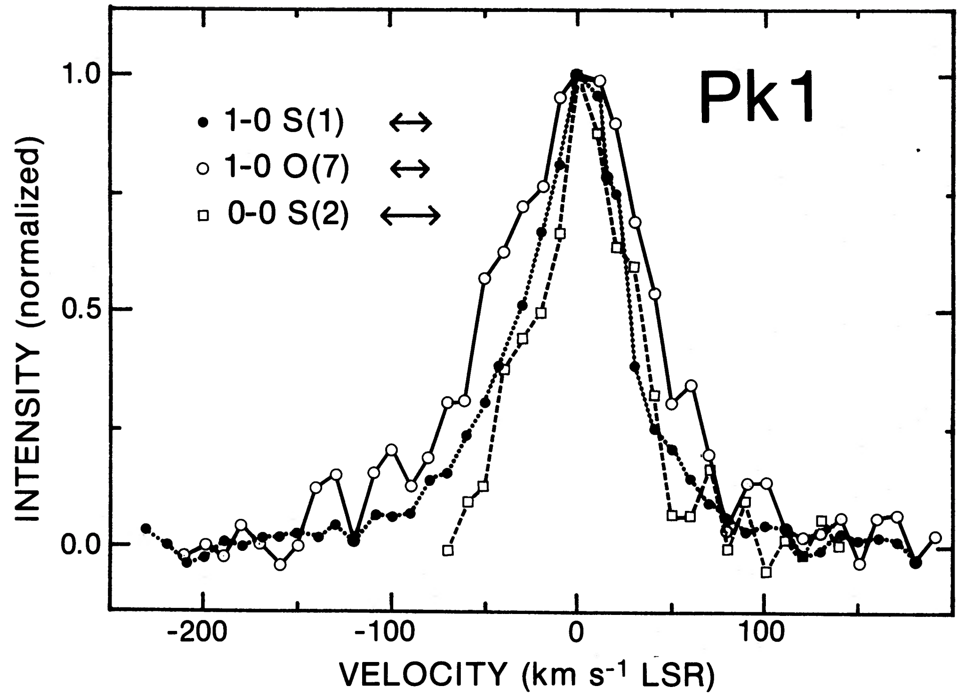

FIG. 2.—Spectra of 1–0 $S(1)$ and $O(7)$ lines and 0–0 $S(2)$ line (obtained by G. Serabyn), all at Peak 1. Beam size was 6″ and velocity resolution 35 km s^{-1} for the $S(2)$ line observations; for the other lines they were 6″.5 and 22 km s^{-1}.

difference between blue and red wing intensities appears to be somewhat less than in the $S(1)$ line, but it is still large. Only at Peak 5 is there an apparent shift in the degree of asymmetry between the two lines; the $O(7)$ line is nearly symmetric. There is no evidence at any of the positions for differences in the extreme velocities in the two lines, although this result is somewhat uncertain because of the low signal-to-noise ratios on the wings of the $O(7)$ lines.

These results appear to contrast somewhat with those of Beck *et al.* (1982), who reported significant differences in the symmetry of profiles of the 12.3 μm $S(2)$ line and the 2.1 μm $S(1)$ line. We note that the interstellar extinctions at 3.8 μm and 12.3 μm are approximately equal (e.g., Rieke and Lebofsky 1985), but that the pure rotational $S(2)$ line is emitted largely by cooler gas than the 1–0 $O(7)$ or $S(1)$ lines. Thus, differences in the $S(2)$ line profiles might be expected to rise from causes other than extinction. At three of the four positions where we have measured the $O(7)$ line, either no $S(2)$ line was detected by Beck *et al.* or the signal-to-noise ratio of their $S(2)$ line is too low to allow the shape to be well characterized. At the other position, Peak 1, their $S(2)$ line appears broader than the $O(7)$ line and rather symmetric. However a more recent and higher signal-to-noise ratio spectrum of the 12.3 μm $S(2)$ line at Peak 1, obtained in 1982 by E. Serabyn, shows that the line has a blue asymmetry relative to $V_{\rm LSR} = 9$ km s^{-1} and is somewhat narrower at half-maximum than either the Beck *et al.* line or the $O(7)$ line. The $S(2)$ line is still quite broad, although lack of baseline prohibits an accurate estimate. This spectrum is shown in Figure 2 along with the $S(1)$ and $O(7)$ spectra at Peak 1.

IV. DISCUSSION

In this section, our goal is to obtain a global picture of the shocked gas region of Orion that is somewhat more detailed than previous pictures. In proceeding toward this goal we rely partially on comparisons of the spectra both at Peak 1, which produced the best $O(7)$ data, and at the other central positions where the lines of sight ought to include all components of a global picture and where the results are similar to those at Peak 1. It must be emphasized, however, that every position for which we have data apparently tells a slightly different story. Until better and more comprehensive data are available, especially for the $O(7)$ line, we do not feel that it is worthwhile to dwell on these differences.

a) Interpretation of the Line Profiles

The result that, with respect to $V_{\rm LSR} = +9$ km s^{-1}, the 3.8 μm $O(7)$ lines and the 2.1 μm $S(1)$ lines have comparable asymmetries at several positions in OMC-1 is important for understanding the morphology of the outflow and the shocked molecular gas there. The previous interpretation that the 2.12 μm $S(1)$ line asymmetries are entirely due to obscuration of redshifted line emission from the far side of the flow by dust within the flow itself predicts that the redshifted emission of the 3.81 μm $O(7)$ line should be nearly as strong as the blueshifted emission, whereas examination of the fractional line strengths in the red and blue channels ($34 < V < 84$ and $-66 < V < -16$) in Table 1 shows that this is not the case for the central three positions, Peak 1, IRc2, and IRc4. Thus, it must be concluded that the line asymmetries reflect in large part the actual line-of-sight distribution of velocities in the shocked gas. Along lines of sight covering much of the line-emitting region, including much of the northern lobe, there is apparently an actual preponderance of blueshifted shocked gas. This interpretation is consistent with the sense of the bipolarity of the molecular outflow in the core of the Orion molecular cloud (Erickson *et al.* 1982).

Nevertheless, there are real differences between the 3.8 μm and 2.1 μm line profiles, which must be explained. At the central three positions, the $O(7)$ lines can be described as fatter (but not wider in their extrema) than the $S(1)$ lines. There are at least two possible explanations for this. One is that the rotational temperature is higher in the high-velocity line-emitting gas than in the low-velocity gas, so that the wings of lines emitted from states of higher J levels are enhanced. Scoville *et al.* (1982) attributed the $\sim$40% higher values of the $S(2)/S(0)$ ratios in the blue wings compared to their core values at Peak 1 and Peak 5 to this effect. A similar increase in both the red and blue wings is found here for the $O(7)/S(1)$ ratio at Peak 1, IRc2, and IRc4. However, if the observed differences between the $S(0)$ (2.22 μm) and $S(2)$ (2.03 μm) profiles, or between the $S(1)$ and $O(7)$ profiles, are wholly attributed to velocity-dependent temperatures, and if the low-velocity line-emitting gas is assigned the standard temperature of 2000 K, the rotational temperature of the wing-emitting gas is required to be $\sim$4000 K. Extinction corrections (*see below*) would imply considerably higher wing temperatures. Such temperatures are unphysically high, because, due to strong dissociation cooling, shocked H_2 radiates in $\Delta V = 1$ lines predominantly in the range 1000–4000 K (Shull and Beckwith 1982). Therefore, we question whether the temperature mechanism is the dominant cause of the line profile differences.

The second explanation is that the line emission at higher velocities is more highly obscured than that at low velocities, so that there is a comparable enhancement of both wings of the $O(7)$ line. It has already been suggested by Chevalier (1980) and by Nadeau, Geballe, and Neugebauer (1982) that H_2–exciting shocks can occur in the molecular outflow itself, which is interior to the low-velocity shock front being driven into the cloud by the outflow (see Fig. 3). If this is the case, the effect of the dust on the $S(1)$ and $O(7)$ line profiles could be as observed, because the high-velocity line emission from the shocks in the flow will be obscured by dust swept up by the flow; this dust lies *between* the low-velocity line emission from the shocked cloud and the flow (see Fig. 3) and thus affects the red and blue wings similarly. We favor the second explanation, which is an extension of that used by Scoville *et al.* (1982) to account for the differences they observed between the $Q(3)$ and $S(1)$ lines (which have the same upper state and thus whose differences cannot be due to temperature). In both cases it is the longer wavelength line of the pair which shows the brighter wing(s). Note that this is the opposite of what Scoville *et al.* observed for the $S(0)$ $S(2)$ pair. There is no way to make all three profile comparisons consistent by invoking velocity-dependent extinction and temperature. We have already pointed out that explanations of the $S(0)$ and $S(2)$ profiles based on temperature are probably unphysical, and we show below that extinction alone is probably sufficient to account for the differences between the $O(7)$ and $S(1)$ profiles. (Indeed, a rotational temperature which is velocity dependent with the opposite sense of that inferred by Scoville *et al.* would make the $O(7)/S(1)$ and $Q(3)/S(1)$ data slightly more consistent.) Although it is clearly important to understand the $S(0)$ and $S(2)$ profiles, because we can think of no straightforward explanation for their ratio which involves temperature and extinction and which is consistent with the higher signal-to-noise $S(1)$, $Q(3)$, and $O(7)$ data, we ignore the $S(0)$ $S(2)$ comparison in the remainder of this paper.

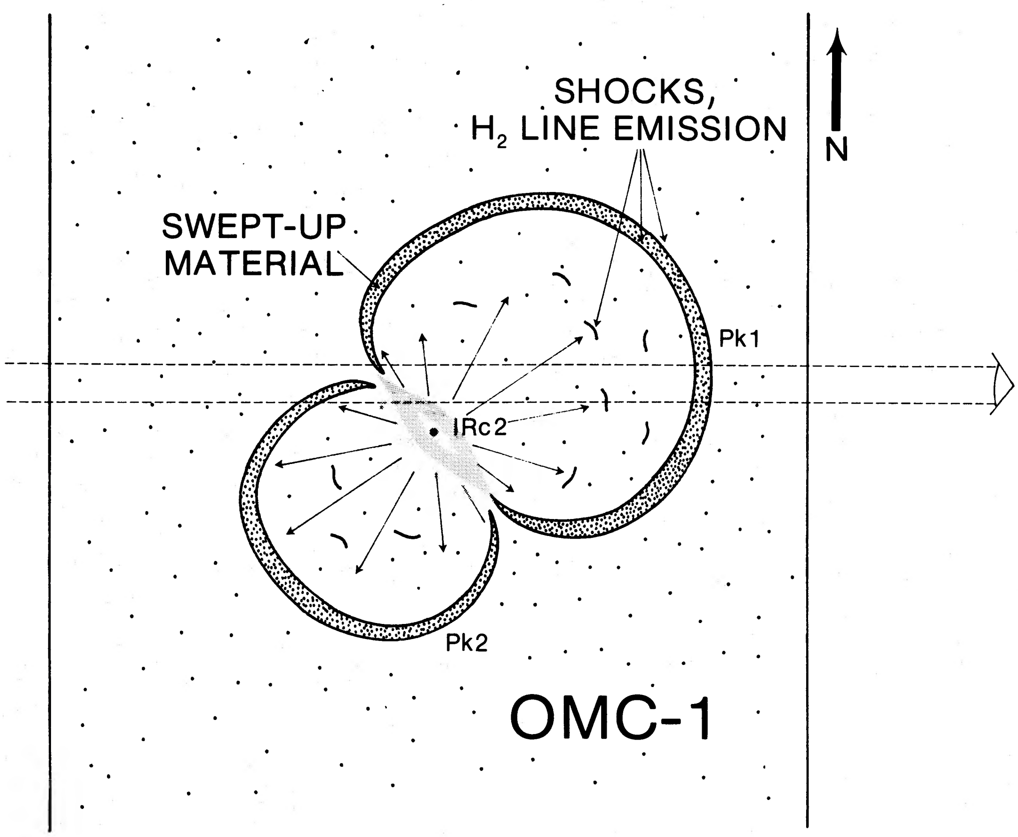

FIG. 3.—Proposed model of the core of OMC-1, as viewed in a slice perpendicular to the E-W axis. Observer views from the right. Outflow source and its dense circumstellar disk are shown at center. Dark arrows indicate protostellar wind. Dust and swept-up molecular cloud are shown. Shock waves which excite H_2 are found both in the protostellar wind and at the interface of the wind and the molecular cloud. Positions of H_2 line peaks are indicated.

TABLE 2

EXTINCTION FROM LOW TO HIGH VELOCITY SHOCKED H_2[a]

$\Delta A_{2.12\,\mu m}$	POSITION				
	Peak 5	Peak 1	IRc2	IRc4	Peak 2
A (blue)–A (low) (mag)[b]	-0.3 ± 0.4	0.6 ± 0.3	0.6 ± 0.3	1.0 ± 0.5	0.0 ± 0.7
A (red)–A (low) (mag)[b]	1.0 ± 0.6	0.6 ± 0.3	0.8 ± 0.6	2 ± 1	0.5 ± 0.5

[a] Assumes $A_\lambda \approx \lambda^{-1.7}$; uses results shown in Table 1.

[b] Blue refers to line emission in velocity interval $-66 < V < -16$, low to $-16 < V < 34$, and red to $34 < V < 84$ (km s^{-1} LSR).

The extinction between the low-velocity gas and the blue-shifted gas resulting from swept-up material can be calculated using the $O(7)$ and $S(1)$ line profiles. We have done so by using the fractional line intensities in the central and adjacent blue-shifted velocity intervals in Table 1, and we have listed the results in Table 2. At the three central positions (Peak 1, IRc2, IRc4) and assuming a rotational temperature which is independent of velocity, the most probable differential extinctions between 3.8 μm and 2.1 μm range from 0.4 to 0.6 mag. Assuming a $\lambda^{-1.7}$ law (Rieke and Lebofsky 1985), the 2.12 μm extinctions from the low-velocity gas to the blue-shifted gas lie in the range 0.6–1.0 mag at 2.1 μm. Scoville *et al.* (1982) also have found evidence in their 1–0 $S(1)$ and $Q(3)$ profiles at Peaks 1 and 5 for increased obscuration of the blue wing, amounting to $\sim$1.7 magnitudes at 2.1 μm. Our extinctions are generally lower than the Scoville *et al.* result, but consistent with it to within the uncertainties. However, at Peak 5 our extinction estimate is discrepant from that of Scoville *et al.*; in fact, we obtain a slightly negative (although, within the uncertainties, indistinguishable from zero) extinction.

The extinctions from the low-velocity gas to the gas emitting the red wing, as derived from the $O(7)$ and $S(1)$ profiles, range from 0.5 to 2.0 mag at 2.1 μm (see Table 2). Although some of the individual values are highly uncertain, as a group they tend to be higher than the extinctions to the blue wing. This result would be expected if the outflow itself contains some dust because the red wing is emitted further along the line of sight. There may also be a contribution to the low-velocity line emission from shocked molecular cloud on the far side of the outflow (see Fig. 3). Because of the high extinction to that region, such a contribution is likely to be very small. However, any contribution will mean that the extinctions to the red and blue wings derived above are underestimated.

The preceding analysis of our data and the Scoville *et al.* (1982) data suggests that $\sim$1 mag of extinction at 2.1 μm occurs in swept-up material between the shocked H_2 in the foreground molecular cloud and the high-velocity outflow. It also suggests that within the outflow itself there is some extinction (0–1 mag at 2.1 μm) which is highly variable with position. This latter extinction is not large enough to account for the blue asymmetries in the 1–0 $S(1)$ line profiles, and thus the profiles must be to large extent intrinsic, as stated above.

b) Scattering

Because many of our spectra have low signal-to-noise ratios, our interpretations of them should be treated with some caution and alternative mechanisms for producing the profiles should be considered. In particular, scattering of line photons by moving grains can modify the intrinsic line shapes. Surrounding the bright northern and southern lobes of $S(1)$ emission in OMC-1, Gatley and Kaifu (1986) have recently detected highly polarized, diffuse, $S(1)$ line emission. They interpret this emission as line radiation scattered by dust in the surrounding molecular cloud. Within the lobes, where we have measured H_2 line profiles, the degree of linear polarization that they and that Joyce and Simon (1982) find in the $S(1)$ line is considerably less. The large-scale alignment of the polarization found by Gatley and Kaifu in the central region is less obviously suggestive of a reflection-nebula mechanism, but it is not yet certain whether this weaker, central polarization is predominantly due to dichroic absorption by foreground dust or whether it is due to scattering by dust moving in the flow itself. If the latter is true, then the emitted line profiles within the lobes may be drastically altered by the dust.

It is not easy, however, to understand both the $S(1)$ and the $O(7)$ line profiles in terms of scattering by moving dust. If scattering from typical-size moving grains causes the broad $S(1)$ lines, the reduced scattering cross section of dust at longer infrared wavelengths implies that the $S(2)$ and the $O(7)$ lines should have substantially *weaker* wings than the $S(1)$ lines. This difference is not observed in the $O(7)$ lines. Comparisons with the $S(2)$ lines are less conclusive; however, they are less important because the $S(2)$ line arises substantially from different gas. Therefore, we tentatively conclude that the bulk of the high-velocity 1–0 $S(1)$, 1–0 $O(7)$, and 0–0 $S(2)$ line photons actually are emitted by high-velocity shocked H_2 molecules. This assertion could be tested directly by measuring the velocity dependence of the polarization of the H_2 lines.

c) A Model of the Outflow and Shocked Gas Region

The infrared H_2 and millimeter CO line profiles in the core of OMC-1 are good indicators of the line-of-sight velocity distributions of the shocked gas and molecular outflow there. One can use them and other data to derive a picture of this region. It is especially important to note several specific characteristics of the line profiles and intensity distributions of H_2, CO, and other molecular lines, as well as infrared continuum and polarization maps. Some of the most important of these characteristics are listed below:

1. The CO millimeter line profiles of Erickson *et al.* (1982), which demonstrate the bipolarity of the outflow, actually show red and blue-shifted wings at each position; it is only a rather modest asymmetry in their line profiles which establishes the bipolarity.

2. A somewhat similar situation occurs for the H_2 line profiles. Those with blue wings are found at declinations almost as far south as Peak 2, further north than Peak 5, and everywhere in between (Nadeau, Geballe, and Neugebauer 1982; Scoville *et al.* 1982). Red wings are found near Peak 1 in the north and Peak 2 in the south, but not in between. The only position where a red asymmetry has been clearly observed is near Peak

2 (see Scoville *et al.*, Fig. 3), whereas blue asymmetries are found over a wide region.

3. Higher blueshifted than redshifted velocities are observed in the H_2 lines; in the CO millimeter lines, the red and blue extrema are approximately equal (± 100 km s^{-1}; e.g., Kwan and Scoville 1976) and comparable to the highest blueshifted velocities seen in H_2 (Nadeau and Geballe 1979).

4. The highest velocities observed in the shocked H_2 lines cannot be actual shock velocities, because as such they would be more than sufficient to dissociate H_2 (Chernoff, Hollenbach, and McKee 1982; Draine, Roberge, and Dalgarno 1983).

5. The peak intensities of the H_2 line profiles always occur at low velocities, within ~ 15 km s^{-1} of the cloud velocity, even at positions where the line profiles are quite broad (Nadeau and Geballe 1979; Scoville *et al.* 1982; Nadeau, Geballe, and Neugebauer 1982; Matsumoto, Moritsugu, and Uyama 1985).

6. The extinctions to the regions of H_2 line wing emission are higher than those to where the line centers are emitted (Scoville *et al.* 1982; this paper).

7. A large, disklike structure of dense gas, whose axis coincides with the direction of the molecular outflow, is present in the core of OMC-1 near the position of IRc2 (e.g., Hasegawa *et al.* 1984).

8. Fundamental-band CO absorption spectroscopy of IRc2 (Geballe and Wade 1985) reveals weak blueshifted absorption, which apparently extends only to -60 km s^{-1} (LSR); this is considerably less than the highest blueshifted velocities observed in either the H_2 or millimeter CO lines.

The following description of the core of OMC-1 is based on the above characteristics and is sketched in Figure 3. A bipolar outflow from IRc2 contains molecular gas moving at velocities of 100 km s^{-1} or more. The outflow is oriented with respect to us, such that its northern lobe lies partly in front of the southern lobe. Gas is ejected by IRc2 along our line of sight at considerably lower velocity than along the axis of the outflow. The outflow has swept up a considerable amount of material from the surrounding molecular cloud; this material is in the form of a thin, dense shell, which is now moving at rather low velocities (perhaps 10–40 km s^{-1}) into the cloud because of its own momentum and that of the impinging outflow. A much larger volume has been swept up by the northern lobe of the outflow than by the southern lobe. Near the outer surface of the shell, ambient molecular cloud material is being shocked, resulting in the widespread, bright line emission by excited H_2 in this rather low-velocity range. Nondissociative (low-velocity) shocks are also present within the outflow and perhaps also at the boundary of the outflow and the swept-up shell; some of the H_2 lines emitted in these shocks occur at high radial velocities in our frame of reference.

The dust in the shell of swept-up material obscures the outflow and the line emission therein. Dust within the outflow itself has the effect of further obscuring the back (redshifted) portion of the outflow. The large disk around IRc2 obscures redshifted infrared line emission from behind it. The presence of the disk helps to explain why so little high-velocity redshifted H_2 line emission is detectable to the south of IRc2. Indeed, it appears that only just a few arc seconds from Peak 2 is there a glimpse of this gas (see Scoville *et al.* 1982, Fig. 3). Line radiation from the shocked molecular cloud on the back side of the outflow is obscured by all of the above and, in addition, by the back side of the shell of swept-up material. It is likely that very little near-infrared line emission from that gas reaches us.

The opening angle of the bipolar outflow from IRc2 likely is quite large, otherwise it probably would not be possible for such a wide range of H_2 radial velocities to be observed over such a large range of positions or for the low-velocity line-emission peak (due to shocked gas at the shell-molecular cloud interface) to be so widespread. The existence of the large disk of gas around IRc2 from millimeter observations and the rather weak and relatively low-velocity CO 4.7 μm fundamental-band absorption observed there imply that the outflow is bipolar at its source. However, the shape of the cavity excavated by a given outflow is determined by existing density inhomogeneities in the surrounding cloud. The shape of the cavity will affect the observed line profiles of both shocked and unshocked gas. Taken as a whole, the H_2 and millimeter molecular line mapping and spectroscopy, together with the infrared CO spectra of IRc2, suggest that both intrinsic flow bipolarity and cloud inhomogeneities have helped to create the present appearance of the outflow region.

The foregoing description accounts for most of the general and some of the specific phenomena associated with the outflow in Orion. Future, more detailed observations will provide important tests of this picture. For example, the different H_2 line profiles must be understood on a position-by-position basis; this will require high-resolution spectroscopy of lines covering a wide range of excitation and wavelength. Clearly it is essential to further test whether the high-velocity H_2 wings are due to actual motions of the shocked gas; this can be accomplished by high-resolution spectropolarimetry and spectroscopy of H_2 lines. Millimeter and submillimeter line measurements at high angular resolution can delineate the extent of the molecular outflow. Finally, it is not clear how the extremely energetic phenomena in Orion, such as the high-velocity Herbig-Haro objects found by Axon and Taylor (1984) fit into the picture. These may be minor events in the evolution of the outflow and its source, or they may require substantial modifications of the present model.

V. SUMMARY

The 3.8 μm $O(7)$ line profiles in the core of OMC-1 generally resemble those of the 2.1 μm $S(1)$ line in their degrees of asymmetry, but have somewhat higher emission in their wings relative to their cores than do the $S(1)$ lines. The increased wing emission indicates that photon scattering off dust grains is not important in producing the wings and argues that the wings arise deeper in the cloud than do the cores of the lines. The data support the presence of line emission at high velocities within the outflow which originates in the BN/KL region.

We wish to thank the staff of Mauna Kea Observatory for its help in obtaining these data. We are grateful to F. Baas for providing the microcomputer for the Fabry-Perot and cold grating spectrometer and to J. Trauger for generous help in coating Fabry-Perot mirrors. We thank E. Serabyn for his spectrum of the $S(2)$ line at Peak 1, and we acknowledge T. B. H. Kuiper for providing a thorough critique of an earlier version of the paper. We also thank Gina Bernabe and S. Yugawa for assistance in preparing the manuscript and figures. This work was supported in part by the National Science Foundation.

REFERENCES

Axon, D. J., and Taylor, K. 1984, *M.N.R.A.S.*, **207**, 241.
Beck, S. C., Bloemhof, E. E., Serabyn, E., Townes, C. M., Tokunaga, A. T., Lacy, J. H., and Smith, H. A. 1982, *Ap. J.* (*Letters*), **253**, L83.
Beckwith, S., Persson, S. E., Neugebauer, G., and Becklin, E. E. 1978, *Ap. J.*, **223**, 464.
Chernoff, D. F., Hollenbach, D. J., and McKee, C. F. 1982, *Ap. J.* (*Letters*), **259**, L97.
Chevalier, R. A. 1980, *Ap. Letters*, **21**, 57.
Draine, B. T., Roberge, W. G., and Dalgarno, A. 1983, *Ap. J.*, **264**, 485.
Erickson, N. R., Goldsmith, P. F., Snell, R. L., Berson, R. L., Huguenin, G. R., Ulich, B. L., and Lada, C. J. 1982, *Ap. J.* (*Letters*), **261**, L103.
Gatley, I., and Kaifu, I. 1986, in *IAU Symposium 120, Astrochemistry*, in press.
Geballe, T. R., and Wade, R. 1985, *Ap. J.* (*Letters*), **291**, L55.
Hasegawa, T., *et al.* 1984, *Ap. J.*, **283**, 117.
Joyce, R. R., and Simon, T. 1982, *M.N.R.A.S.*, **200**, 39P.
Kwan, J., and Scoville, N. Z. 1976, *Ap. J.* (*Letters*), **210**, L39.
Matsumoto, T., Moritsugu, T., and Uyama, K. 1985, *Pub. Astr. Soc. Japan*, **37**, 129.
Nadeau, D., and Geballe, T. R. 1979, *Ap. J.* (*Letters*), **230**, L169.
Nadeau, D., Geballe, T. R., and Neugebauer, G. 1982, *Ap. J.*, **253**, 154.
Persson, S. E., Geballe, T. R., and Baas, F. 1982, *Pub. A.S.P.*, **94**, 381.
Rieke, G. H., and Lebofsky, M. J. 1985, *Ap. J.*, **288**, 618.
Scoville, N. Z., Hall, D. N. B., Kleinman, S. G., and Ridgway, S. T. 1982, *Ap. J.*, **253**, 136.
Shull, J. M., and Beckwith, S. 1982, *Ann. Rev. Astr. Ap.*, **20**, 163.
Zuckerman, B., Kuiper, T. B. M., and Rodriguez Kuiper, E. N. 1976, *Ap. J.* (*Letters*), **209**, L13.

T. R. GEBALLE: United Kingdom Infrared Telescope, 665 Komohana Street, Hilo, HI 96720

CAROL J. LONSDALE: IPAC, Caltech 100-22, Pasadena, CA 91125

P. J. MCGREGOR: Mount Stromlo and Siding Spring Observatories, Private Bag, P.O. Woden ACT 2606, Australia

S. E. PERSSON: The Observatories, 813 Santa Barbara Street, Pasadena, CA 91101

THEODORE SIMON: Institute for Astronomy, University of Hawaii, 2680 Woodlawn Drive, Honolulu, HI 96822